

# Coherent control of electron localization in a dissociating hydrogen molecular ion

Feng He and Andreas Becker

Max-Planck-Institut für Physik komplexer Systeme, Nöthnitzer Str 38, D-01187 Dresden, Germany

Received 20 September 2007, in final form 18 January 2008

Published 25 March 2008

Online at [stacks.iop.org/JPhysB/41/074017](http://stacks.iop.org/JPhysB/41/074017)

## Abstract

We have performed *ab initio* numerical simulations of the time-dependent Schrödinger equation of the hydrogen molecular ion interacting with one or two (time-delayed) ultrashort laser pulses. Dissociation of the molecular ion is analysed in view of an asymmetry in the electron localization on the two protons. The results show that the asymmetry is most effectively induced by the external field as the dissociating nuclei reach a critical internuclear distance, at which the interatomic barrier inhibits an oscillation of the electron between the nuclei. Different schemes, proposed previously to control the electron dynamics and its localization in the molecular bond, are compared in view of the present results.

(Some figures in this article are in colour only in the electronic version)

## 1. Introduction

Ultrashort flashes of light generated by intense laser sources are an important tool to observe and control electronic and nuclear motion in atoms and molecules. Using femtosecond laser pulses it has become possible to visualize the breaking and rearrangement of bonds in a molecular system [1, 2]. Different strategies have been proposed and realized to maximize or minimize the probability of a certain reaction channel on the femtosecond time scale [3, 4]. Prominent examples are based on the interference between different pathways to a final channel [5], the time delay between two laser pulses [6, 7] or the manipulation of the spectral phases and amplitudes of the different frequency components of the pulse [8, 9].

Recent technological development of few-cycle laser pulses with a controlled carrier-envelope phase and attosecond pulses and pulse trains [10–12] has paved the way to extend the control from the time scale of nuclear motion to that of the electrons in atoms and molecules. This has been demonstrated by the observation of asymmetries in the photoelectron angular distribution from atoms [13, 14] and molecules [15, 16] as well as in the products of molecular dissociation [17–21]. The latter studies are of particular interest in view of the application of ultrashort laser pulses to control the products of a chemical reaction as they manifest subfemtosecond control of electron dynamics in a molecular bond. Two control schemes have been proposed recently to drive an electron in a dissociating molecule and localize it purposefully on one

of the products of the dissociation. First, a steering of the electron has been achieved via the phase between the envelope and the carrier frequency of a single few-cycle laser pulse. In numerical simulations, an asymmetry in the ejection of the ionic fragments in the dissociation of  $H_2^+$  and  $HD^+$  has been found to depend on the carrier-envelope phase of the pulse [17]. The ansatz has been successfully applied in an experiment on  $D_2$  [18] followed by theoretical analysis of the experimental observations [19, 21]. In a second strategy two time-delayed coherent laser pulses are used to control the localization of the electron during the dissociation of  $H_2^+$  and its isotopes [20]. In *ab initio* numerical simulations it has been shown that the first (sub-)femtosecond ultraviolet pulse excites the electron wave packet on the dissociative  $2p\sigma_u$  state, while the second near-infrared pulse steers the electron between the two dissociating nuclei. A high localization probability of about 85% is found using the two-pulse control scheme.

In order to maximize the extent of electron localization in a molecular bond and to apply the control schemes to other molecules, it is important to understand the quantum dynamics behind the control in the simplest molecules  $H_2^+$  and its isotopes. It has been shown in the past that these molecules play an important role in understanding ultrafast phenomena in molecules in general, since they can be studied in experiment as well as in *ab initio* numerical simulations. The combined experimental and theoretical effort has, e.g., revealed a number of possible channels to dissociation and dissociative ionization in a single laser pulse, such as above threshold dissociation [22], bond softening [23, 24], bond

hardening [25], charge-resonant enhanced ionization [26, 27] or above threshold Coulomb explosion [28]. Considering the control of electron localization it has been argued [18, 20] that the rising interatomic barrier between the two dissociating nuclei in  $\text{H}_2^+$  or one of its isotopes plays an important role. Any (laser-driven) oscillation of the electron between the two nuclei has to cease as soon as this barrier can no longer be overcome by the electron. Thus, it is likely that the control of the electron dynamics in the current proposals is most effective when the dissociating nuclei are at a critical distance  $R_c$ , at which the interatomic barrier reaches the energy of the dissociative  $2p\sigma_u$ -state.

In this paper, we further analyse the mechanism for coherent control of electron localization during the dissociation of the hydrogen molecular ion. To this end, we have performed a series of numerical simulations using a three-dimensional non-Born–Oppenheimer model for  $\text{H}_2^+$  interacting with intense linearly polarized laser pulses. The model used for the simulations will be presented in the following section. In section 3, we consider the interaction of the molecular ion with laser pulses having a constant amplitude but different number of cycles. The results will confirm the previous expectations that the electron dynamics is most effectively controlled by the electric field as the dissociating nuclei reach the critical distance  $R_c$ . We will then proceed in section 4 by investigating the electron wave packet dynamics and the extent of electron localization in the two different control schemes proposed up to now. The paper ends with a short summary.

## 2. Three-dimensional non-Born–Oppenheimer model of $\text{H}_2^+$

A solution of the time-dependent Schrödinger equation of the hydrogen molecular ion interacting with an intense laser pulse would require the propagation of a six-dimensional wavefunction with three degrees of freedom for the electron as well as the nuclei dynamics. This is at the limit of current computer capacities. Therefore, in practice the system is usually studied in models of reduced dimensions, which however retain the essential physics of the problem of interest. We have used for our numerical simulations a three-dimensional model including nuclear vibrations along the internuclear axis and two electronic degrees of freedom [17, 20, 29, 30]. The time-dependent Schrödinger equation of this model is given by (Hartree atomic units,  $e = m = \hbar = 1$  are used):

$$i \frac{\partial}{\partial t} \Phi(R, z, \rho; t) = [H_0 + V(t)] \Phi(R, z, \rho; t). \quad (1)$$

Here,  $H_0$  is the field-free Hamiltonian

$$H_0 = -\frac{1}{2\mu} \frac{\partial^2}{\partial R^2} - \frac{1}{2\mu_e} \left( \frac{\partial^2}{\partial z^2} + \frac{\partial^2}{\partial \rho^2} + \frac{1}{\rho} \frac{\partial}{\partial \rho} \right) + \frac{1}{\sqrt{R^2 + \beta}} - \frac{1}{\sqrt{(z - R/2)^2 + \rho^2 + \alpha}} - \frac{1}{\sqrt{(z + R/2)^2 + \rho^2 + \alpha}}, \quad (2)$$

where  $R$  is the internuclear distance and  $\mu = m_p/2$  and  $\mu_e = 2m_p/(2m_p + 1)$  are the reduced masses,  $m_p$  is the mass

of the proton. The parameters  $\alpha = 0.0109$  and  $\beta = 0.1$  are introduced to soften the Coulomb interactions. The values are chosen such that the model yields the experimental ground state energy and equilibrium distance of  $-0.6028$  au and  $2.0$  au of the hydrogen molecular ion, respectively.  $V(t)$  takes account of the interaction of the electron with one or two (time-delayed) linearly polarized intense laser pulses:

$$V(t) = [E_1(t) + E_2(t - \Delta t)]z. \quad (3)$$

The electric fields are chosen to be linearly polarized along the internuclear axis and are given by  $E_i(t) = E_{0,i} f(t) \sin(\omega_i t)$ , where  $\omega_i$  is the frequency and  $E_{0,i}$  is the peak amplitude of the  $i$ th pulse. In the present simulations we have considered one or two pulses with either a constant amplitude over  $N$  cycles of the field or a Gaussian shape,  $f(t) = \exp[-8 \ln 2 (t/\tau)^2]$ , where  $\tau$  is the pulse duration (full width at half-maximum, FWHM). In case two pulses are used  $\Delta t$  is the time delay between them.

The three-dimensional model accounts for non-Born–Oppenheimer effects and applies for an interaction of the molecular ion with laser pulses of linear polarization, where the internuclear axis of the molecule is oriented along the polarization axis of the laser. In an experiment with an ensemble of randomly oriented molecules such events can be usually identified from the direction in which the protons are detected. In the model any rotation of the molecule during the interaction with the external pulses is not taken into account, since it is expected that the molecules do not rotate significantly over a few tens of femtoseconds.

The time-dependent Schrödinger equation (1) has been solved on a grid with 500 points in the  $R$ -direction ( $R = [0 \text{ au}, 20 \text{ au}]$ ), 200 and 80 points in the  $z$ - and  $\rho$ -directions, respectively ( $z = [-30 \text{ au}, 30 \text{ au}]$ ,  $\rho = [0 \text{ au}, 24 \text{ au}]$ ) and a time step of  $\delta t = 0.05$  au using the Crank–Nicholson method. Absorbing boundaries at the edges of the grid are employed using  $\cos^{1/6}$ -masking functions. We have considered the electronic  $1s\sigma_g$  and vibrational  $v = 0$  ground state of the model hydrogen molecular ion, which has been obtained by imaginary time propagation. In order to distinguish the two different channels of dissociation, i.e. the electron localization at either one of the two dissociating protons, we have separated the coordinate space such that

$$P_+ : R > 10 \quad \text{and} \quad \sqrt{(z - R/2)^2 + \rho^2} < 5, \quad (4)$$

$$P_- : R > 10 \quad \text{and} \quad \sqrt{(z + R/2)^2 + \rho^2} < 5, \quad (5)$$

where  $P_+$  and  $P_-$  are defined as the integrals of the probability density over the respective regions. They account for the probabilities of directional localization of the electron along the positive and negative  $z$ -axis, respectively. Contributions absorbed at the edges of the grid during the propagation of the wavefunction are added to the respective channels of dissociation. The wavefunction has been propagated until the probabilities for all reaction channels are converged. A dissociation asymmetry in the electron localization along the positive and negative  $z$ -direction has been defined as

$$A = \frac{P_- - P_+}{P_- + P_+}. \quad (6)$$

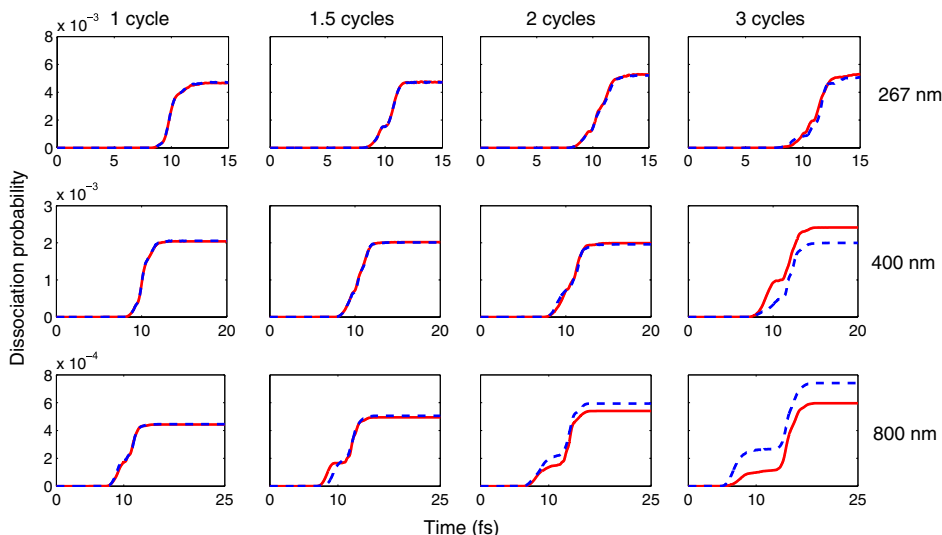


**Figure 1.** Dissociation probabilities  $P_+$  (blue dashed line) and  $P_-$  (red solid lines) for the interaction of  $\text{H}_2^+$  with a laser pulse of constant amplitude as a function of time. Results presented in the same row are obtained at the same wavelength, while those shown in the same column are due to interaction with a pulse of the same number of cycles. The laser intensities are  $10^{14} \text{ W cm}^{-2}$ ,  $10^{14} \text{ W cm}^{-2}$  and  $3 \times 10^{14} \text{ W cm}^{-2}$  for 267 nm, 400 nm and 800 nm, respectively.

### 3. Origin of electron localization asymmetry during dissociation

In order to understand the origin of the asymmetry of electron localization during the laser-driven dissociation of  $\text{H}_2^+$  we have first performed a set of simulations in which one pulse of constant amplitude interacts with the hydrogen molecular ion. Such pulses with a rectangular shape and a constant intensity provide an accurately defined time interval of interaction with the external field. As will be shown below, it will allow us to distinguish the excitation of the electron wave packet and its control in the dissociating molecular ion. Furthermore, the time interval between the two steps can be determined more accurately as, e.g., in a Gaussian laser pulse, which has tails at lower intensities. In the simulation the frequency and the number of cycles of the pulse are varied. Figure 1 shows the dissociation probabilities as a function of time for different wavelengths between 267 nm (first row) and 800 nm (last row) and 1 (left-hand column) to 3 (right-hand column) number of cycles in the pulse. The origin of the time axis is set at the centre of the respective laser pulse. The red solid and blue dashed lines represent the dissociation probabilities  $P_-$  and  $P_+$ , respectively (cf equations (4) and (5)). Constant laser intensities have been chosen as  $10^{14} \text{ W cm}^{-2}$ ,  $10^{14} \text{ W cm}^{-2}$  and  $3 \times 10^{14} \text{ W cm}^{-2}$  for 267 nm, 400 nm and 800 nm, respectively.

The results in the figure show that the first part of the dissociative wave packet needs about 10 fs to reach the domains defined as dissociation channels in the simulation. Furthermore, the probabilities are found to converge towards the end of the simulations. Most interesting in the present context is that for all three laser frequencies there is no asymmetry in the electron localization found for the shortest pulse durations. However, as the number of cycles in the pulses increases, differences between the probabilities for the two

dissociation branches occur and increase with further increase of the pulse duration. The minimum number of cycles needed to achieve an asymmetry in the electron localization changes from 1.5 cycles in the case of a 800 nm driving pulse to 3 cycles for a wavelength of 267 nm.

The results in figure 1 indicate two key points in view of the origin of the asymmetry in the final electron localization. First, the observed asymmetry is not induced by the initial step of dissociation, i.e. the excitation to the dissociative  $2p\sigma_u$ -state. This conclusion can be drawn from the fact that we do observe dissociation but no asymmetry in the two dissociation channels for the shortest pulse durations. Thus, the asymmetry has to occur due to the interaction with the field during the dissociation of the two nuclei. Second, it is likely that the dissociating nuclei have to be separated by a certain critical distance as the asymmetry is induced, since the minimum number of cycles needed to obtain a difference between the electron localization in the two channels varies with the wavelength of the driving pulse. The two points are in agreement with the conclusions of previous studies [18, 20] that a control of the electron dynamics by the field is most effective at internuclear distances at which the interatomic Coulomb barrier reaches the energy of the dissociative  $2p\sigma_u$ -state.

Further insights can be gained from the evolution of the probability density,  $P(R, t) = \iint |\Phi(R, z, \rho; t)|^2 dz d\rho$ , as a function of time  $t$  and internuclear distance  $R$ , as plotted in the lower rows of figures 2 (for pulses at 400 nm) and 3 (for pulses at 800 nm). Note that the probability densities are given on a logarithmic scale with a colour coding in powers of 10. The panels in the different columns show the results of the numerical simulations for interaction with a 1- (left-hand column), 2- (middle column) and 3-cycle pulse (right-hand column), respectively. To guide the eye the electric fields of

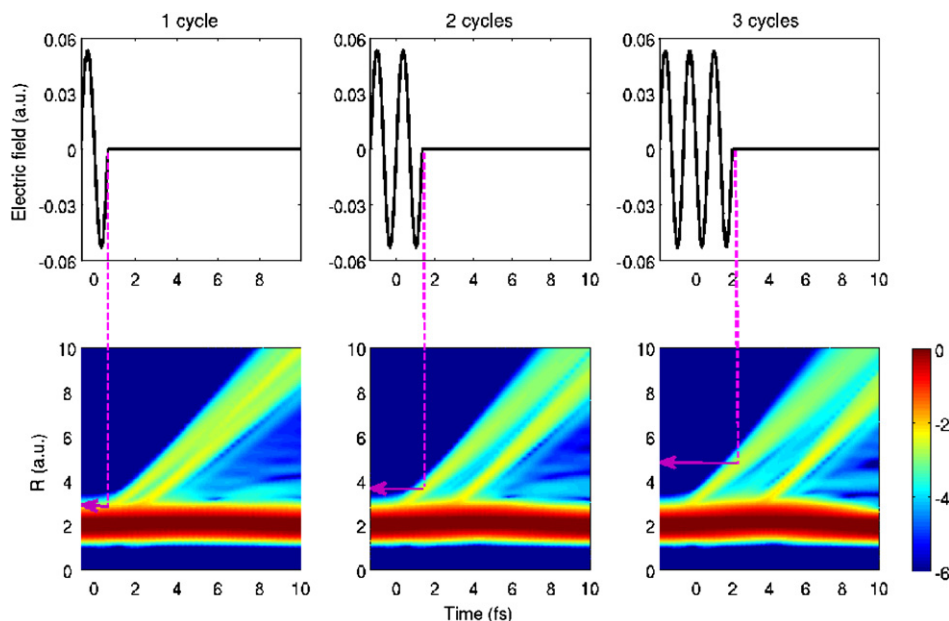


**Figure 2.** Electric field (upper row) as function of time and probability density  $P(R, t)$ , integrated over the two electron coordinates, as a function of time and the internuclear distance (lower row, given on a logarithmic scale). Results are shown for simulations at 400 nm and a constant laser intensity of  $10^{14} \text{ W cm}^{-2}$ . Pulse durations are 1 cycle (left-hand column), 2 cycles (middle column) and 3 cycles (right-hand column).

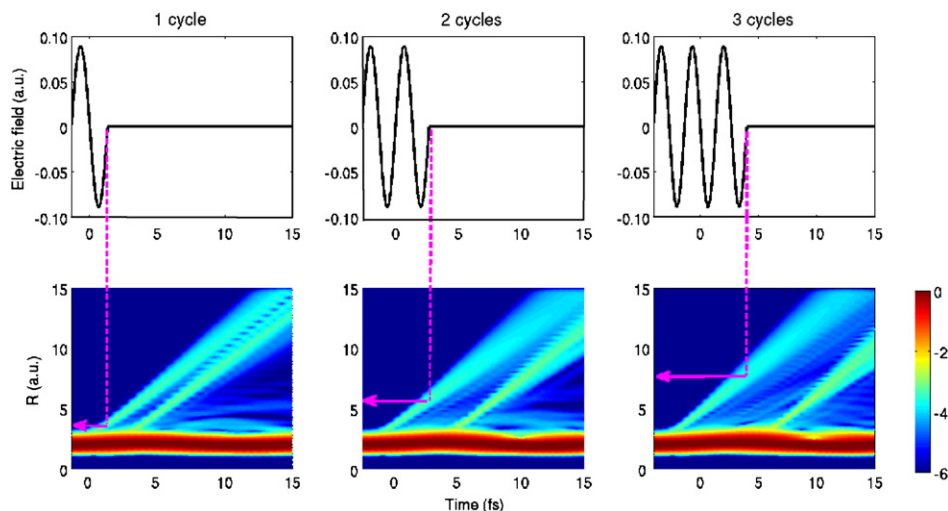


**Figure 3.** Same as figure 2 but for 800 nm and  $3 \times 10^{14} \text{ W cm}^{-2}$ .

the corresponding laser pulses as a function of time are plotted in the upper row of each column.

In all cases shown, initially, the wave packets are located around  $R = 2$ , which is the equilibrium distance for the vibrational ground state of  $H_2^+$ . As can be seen from the figure the major part of the probability density remains bound in the vibrational ground state while smaller parts start to propagate to larger internuclear distance, indicating dissociation of the molecular ion. Please note that there are two major dissociation events, caused by the sudden turn-on and turn-off of the rectangular pulse. The sudden change in the electric field acts as an attosecond pulse, which initiates

the dissociation. These artificial effects, which are not seen in the results obtained with a realistic Gaussian laser pulse (cf figures 5 and 6), allow us to accurately determine the moments of excitation (and control) of the electron wave packets. We may note parenthetically that somewhat similar effects induced by a rectangular pulse shape have also been noticed in ionization of atoms [31]. Some other small parts of the density remain at constant internuclear distances larger than the equilibrium distance. The latter parts are due to excitation in higher vibrational states of the molecular ion, which are of no relevance in the present context.

We now turn to the question at which internuclear distance an asymmetry of the electron localization in the dissociative wave packet can be induced by the field. To this end, we have marked the time at which the corresponding driving field vanishes by dashed lines in each of the columns of figures 2 and 3. As expected, the longer is the pulse duration the larger is the internuclear distance, at which the dissociative wave packet is found at the end of the pulse (indicated by the arrow in each of the panels). Recalling that an asymmetry in the final electron localization has been found for a minimum of 3 and 1.5 cycles of the field at 400 nm and 800 nm, respectively (cf figure 1), we may infer from the present results a minimum internuclear distance of 4–5 au for the dissociative wave packet to induce the asymmetry effectively. In the present model the interatomic Coulomb barrier reaches the energy of the  $2p\sigma_u$  at an internuclear distance of  $R_c = 6.3$  au. Thus, the above results indicate that the electron wave packet is driven by the field towards one nucleus during one half cycle before the interatomic barrier inhibits the free oscillation of the electron wave packet between the nuclei and the wave packet gets localized preferably at one of the two protons.

We have further tested our interpretation by applying a second ultrashort weak laser pulse with a certain time delay to the first pulse. We have considered two cases, in which the initial pulse did not induce an asymmetry in the final electron localization, namely one- and two-cycle pulses at 400 nm (cf figure 1). We have chosen the parameters of the second pulse such that it does not induce any additional dissociation of the molecular ion (weak constant laser intensity of  $3 \times 10^{12}$  W cm $^{-2}$ ) and its application is restricted in time (pulse duration of one cycle at 400 nm). In view of the above results we expect to observe an asymmetry in the electron localization if the second pulse is applied over a certain time window during which the dissociative wave packet is located at internuclear distances of about  $R_c = 6.3$  au. The results of our numerical simulations for the asymmetry parameter  $A$  are shown in figure 4, which indeed confirm our expectations. The electron localization can be controlled over a time window between 3 fs and 8 fs, which corresponds to the expected localization of parts of the dissociative wave packet in the region of 6.3 au (cf figure 2, left-hand and middle panels in the lower row).

The results presented above therefore confirm the conclusion of previous studies [18, 20] that the interatomic Coulomb barrier between the protons plays a decisive role for the electron localization during the dissociation of  $H_2^+$  (and its isotopes). In this respect a critical internuclear distance  $R_c$  is given by the point at which the interatomic barrier reaches the energy of the dissociative  $2p\sigma_u$  state. The oscillation and final localization of the electron can be most effectively influenced by an external electric field, which is applied during the time window at which the dissociative wave packet passes  $R_c$ . In the following section we will compare the two strategies proposed to control the electron localization in view of these conclusions.

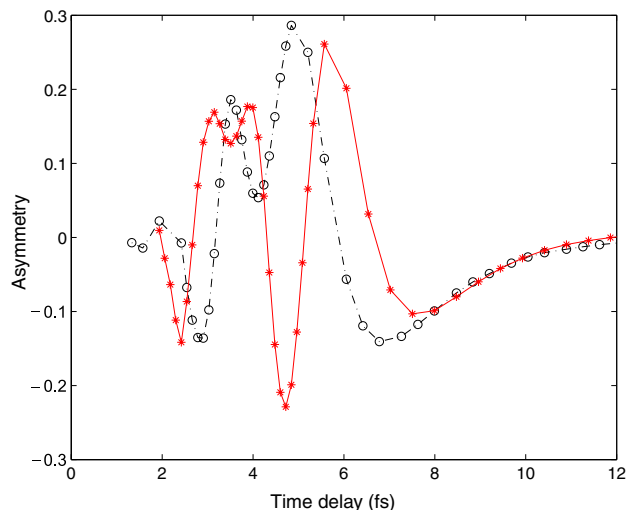


**Figure 4.** Asymmetry parameter  $A$  of the electron localization as a function of the time delay between two laser pulses at 400 nm and constant laser intensities of  $10^{14}$  W cm $^{-2}$  and  $3 \times 10^{12}$  W cm $^{-2}$ , respectively. Pulse durations were 1 (solid line with stars) and 2 cycles (dashed line with circles) for the first pulse and 1 cycle for the second pulse.

#### 4. Control of electron localization with one and two laser pulses

The results in the previous sections have been obtained with unrealistic ultrashort laser pulses having a constant intensity. They however provided further insights into the mechanism of electron localization during the dissociation of the hydrogen molecular ion. We now turn to the two control schemes, proposed before in the literature [17, 20], which are feasible on the basis of the current laser technology.

As already outlined at the outset in the first proposal [17] a control of the asymmetry in the electron localization between the two protons has been achieved via the carrier–envelope phase of a single rather long near-infrared pulse (Gaussian shape with 10 fs FWHM). Considering the results of the previous section the laser pulse is certainly long enough that its tail does steer the electron as the dissociative wave packet reaches the critical internuclear distance. We may expect that the asymmetry in the electron localization disappears if the laser pulse is shortened. To test our expectations we have performed simulations with Gaussian laser pulses at 400 nm central wavelength with pulse durations (FWHM) of 2 ( $\tau = 2.6$  fs) and 6 cycles ( $\tau = 7.8$  fs), respectively. The peak laser intensity was  $5 \times 10^{14}$  W cm $^{-2}$  in both cases. The corresponding results for the probabilities in the two dissociation channels,  $P_-$  (red solid line) and  $P_+$  (blue dashed line), are presented in the upper row of figure 5 along with the probability densities  $P(R, t)$  in the lower row. As expected, for the shorter pulse the probabilities for electron localization at both nuclei are identical, since the field vanishes too quickly to induce an effective control. We have further found that this result is independent of the carrier–envelope phase of the pulse (not shown). On the other hand, an asymmetry in the electron localization is observed for a pulse length of

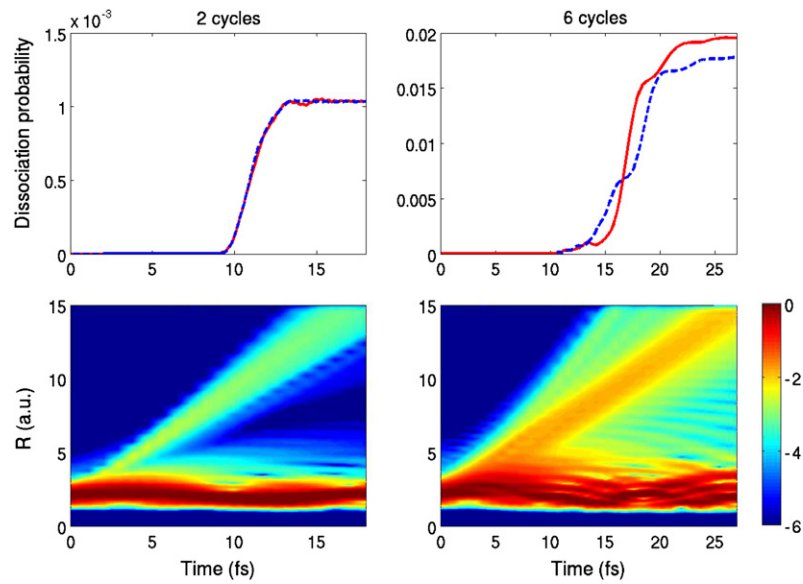


**Figure 5.** Upper row: dissociation probabilities  $P_-$  (red solid line) and  $P_+$  (blue dashed line) as a function of time. Lower row: probability densities  $P(R, t)$ , given on a logarithmic scale, as a function of time and internuclear distance. Results are presented for interaction with Gaussian laser pulses at 400 nm and a peak intensity of  $5 \times 10^{14} \text{ W cm}^{-2}$  with FWHM pulse durations of 2 cycles (left column) and 6 cycles (right column).

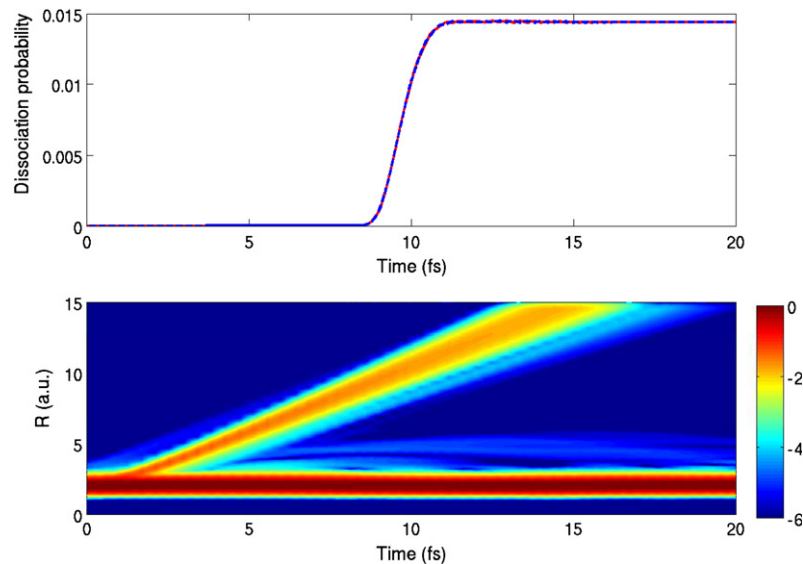


**Figure 6.** Same as figure 5 but for different laser parameters. Here the central wavelength of the laser pulse is 106 nm with a peak intensity of  $10^{13} \text{ W cm}^{-2}$  and FWHM pulse duration of 2 cycles.

6 cycles. Here the pulse is long enough to steer the electron as the nuclei reach the critical internuclear distance leading to an asymmetric localization. It is the strength and the carrier-envelope phase which determines the extent of the asymmetry, as has been found in the previous studies [17, 18].

In case of the longer pulse the probability density  $P(R, t)$  shows a rather broad distribution, which is caused by two effects. Since the laser pulse contains a few cycles, several dissociative wave packets are created. On the other hand, dissociation occurs via different pathways and the sub-wave packets overlap during further propagation. It is therefore

not very likely that the resulting widely spread dissociative wave packet can be controlled to a high degree as it passes the critical internuclear distance.

To obtain a high degree of control of the electron localization, it is therefore desirable to confine the dissociative wave packet as much as possible. This is achieved in the two-pulse control scheme proposed recently [20]. In that case a first attosecond laser pulse is used to excite an electron wave packet via a one-photon transition on the dissociative  $2p\sigma_u$  state. As can be seen from the results in figure 6 this ultrashort pulse (106 nm,  $10^{13} \text{ W cm}^{-2}$ ,  $\tau = 0.7 \text{ fs}$ ) does not induce

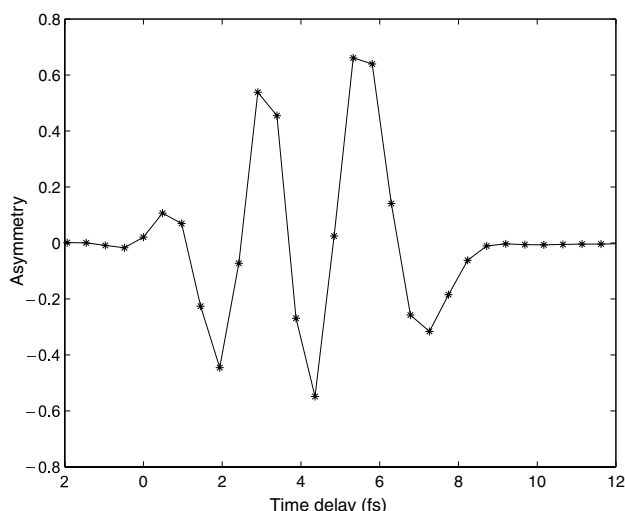


**Figure 7.** Same as figure 4 but for different laser parameters. The parameters of the first laser pulse are the same as in figure 6. The wavelength, peak intensity and pulse duration of the second steering laser pulse are 800 nm,  $5 \times 10^{12}$  W cm $^{-2}$  and 5.2 fs, respectively.

any asymmetry in the final electron localization but a rather well-confined wave packet in the dissociation channel. This allows to control the asymmetry in the electron localization with a second time-delayed laser pulse to a high degree. It is demonstrated by the results for the asymmetry parameter  $A$  as a function of time delay between the two pulse presented in figure 7. The results are obtained with a second near-infrared laser pulse at 800 nm,  $5 \times 10^{12}$  W cm $^{-2}$  and  $\tau = 5.2$  fs. It has been shown [20] that in this control scheme the electron localization is sensitive to the time delay and the carrier-envelope phase of the second laser pulse. An effective control is achieved for time delays between 2 fs and 8 fs with a maximum asymmetry of 84% in the  $P_-$  channel at  $\Delta t = 5.3$  fs.

## 5. Conclusions

We have analysed the origin of an asymmetry in the electron localization during the laser-induced dissociation of  $H_2^+$ . Results of numerical simulations have shown that the asymmetry is not induced during the excitation to the dissociative state but during the dissociation of the molecular ion to larger internuclear distances. It has been found that a control of the electron dynamics between the two protons is most effective, if an external field is applied when the protons reach a critical internuclear distance. This distance is determined by the point at which the interatomic Coulomb barrier reaches the energy of the dissociative state. A comparison of two control strategies, namely via the carrier-envelope phase of a single laser pulse and via two time-delayed pulses, has revealed that the latter is more effective due to the

stronger confinement of the dissociative wave packet at the critical internuclear distance.

## Acknowledgments

We thank C Ruiz for fruitful discussions. The present results are obtained using the Virtual Laser Lab NPSFLIB; contributions by S Baier, P Panek, A Requate and C Ruiz are acknowledged.

## References

- [1] Zewail A H 2000 *J. Phys. Chem. A* **104** 5660
- [2] Hertel I V and Rodloff W 2006 *Rep. Prog. Phys.* **69** 1897
- [3] Rice S A and Zhao M 2000 *Optimal Control of Molecular Dynamics* (New York: Wiley-Interscience)
- [4] Shapiro M and Brumer P 2003 *Principles of the Quantum Control of Molecular Processes* (New York: Wiley)
- [5] Shapiro M and Brumer P 1986 *J. Chem. Phys.* **84** 4103
- [6] Tannor D J and Rice S A 1985 *J. Chem. Phys.* **83** 5013
- [7] Tannor D J, Kosloff R and Rice S A 1986 *J. Chem. Phys.* **85** 5805
- [8] Judson R S and Rabitz H 1992 *Phys. Rev. Lett.* **68** 1500
- [9] Assion A, Baumert T, Bergt M, Brixner T, Kiefer B, Seyfried V, Strehle M and Gerber G 1998 *Science* **282** 919
- [10] Kienberger R *et al* 2004 *Nature* **427** 817
- [11] Goulielmakis E *et al* 2004 *Science* **305** 1267
- [12] Hauri C P, Kronelis W, Helbing F W, Heinrich A, Couairon A, Mysyrowicz A, Biegert J and Keller U 2004 *Appl. Phys. B* **79** 673
- [13] Paulus G G, Grasbon F, Walther H, Villoresi P, Nisoli M, Stagira S, Prori E and Silvestri S De 2001 *Nature* **414** 182
- [14] Lindner F, Schätzel M G, Walther H, Baltuska A, Goulielmakis E, Krausz F, Milosevic D B, Bauer D, Becker W and Paulus G G 2005 *Phys. Rev. Lett.* **95** 040401
- [15] Bandrauk A D, Chelkowski S and Nguyen H S 2000 *Int. J. Quantum Chem.* **100** 834
- [16] Chelkowski S, Yudin G L and Bandrauk A D 2006 *J. Phys. B: At. Mol. Opt. Phys.* **39** S409
- [17] Roudnev V, Esry B D and Ben-Itzhak I 2004 *Phys. Rev. Lett.* **93** 163601
- [18] Kling M F *et al* 2006 *Science* **312** 246
- [19] Tong X M and Lin C D 2007 *Phys. Rev. Lett.* **98** 123002
- [20] He F, Ruiz C and Becker A 2007 *Phys. Rev. Lett.* **99** 083002
- [21] Gräfe S and Ivanov M 2007 *Phys. Rev. Lett.* **99** 163603
- [22] Giusti-Suzor A, He X, Atabek O and Mies F H 1990 *Phys. Rev. Lett.* **64** 515
- [23] Bandrauk A D and Sink M L 1981 *J. Chem. Phys.* **74** 1110
- [24] Bucksbaum P H, Zavriyev A, Muller H G and Schumacher D W 1990 *Phys. Rev. Lett.* **64** 1883
- [25] Fransinski L J, Posthumus J H, Plumridge J, Codling K, Taday P F and Langley A J 1999 *Phys. Rev. Lett.* **83** 3625
- [26] Zuo T and Bandrauk A D 1995 *Phys. Rev. A* **52** R2511
- [27] Seideman T, Ivanov M Yu and Corkum P B 1995 *Phys. Rev. Lett.* **75** 2819
- [28] Esry B D, Saylor A M, Wang P Q, Carnes K D and Ben-Itzhak I 2006 *Phys. Rev. Lett.* **97** 013003
- [29] Kamta G Lagmago and Bandrauk A D 2005 *Phys. Rev. Lett.* **94** 203003
- [30] Bandrauk A D, Barmaki S and Kamta G Lagmago 2007 *Phys. Rev. Lett.* **98** 013001
- [31] Bauer D and Mulser P 1999 *Phys. Rev. A* **59** 569